3CLpro and PLpro affinity, a docking study to fight COVID19 based on 900 compounds from PubChem and literature. Are there new drugs to be found?

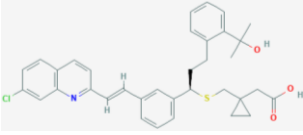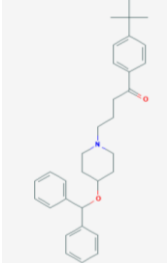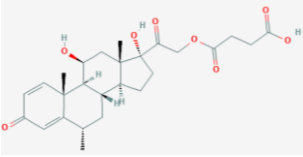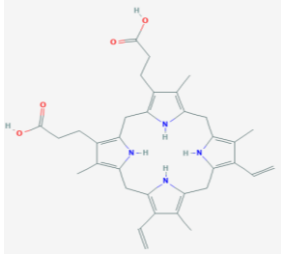**Marek Štekláč,[1] Dávid Zajaček[1] and Lukáš Bučinský[1]**
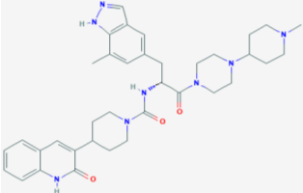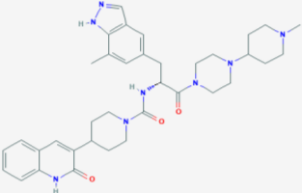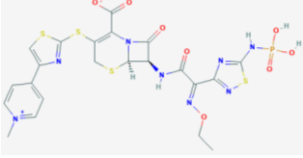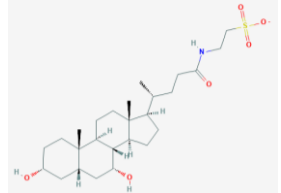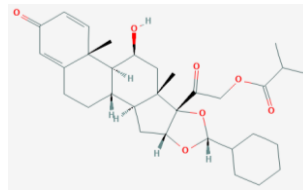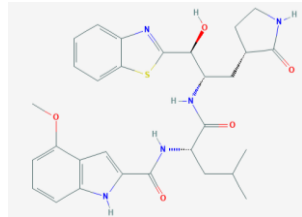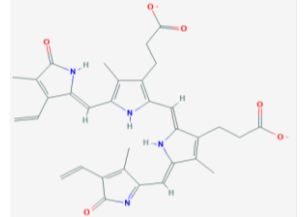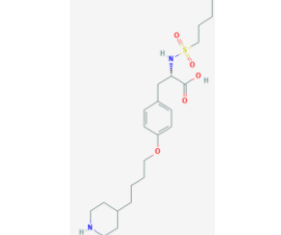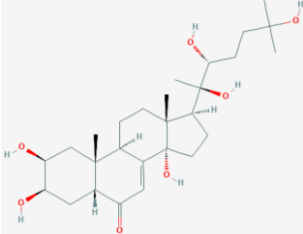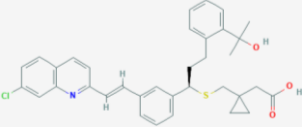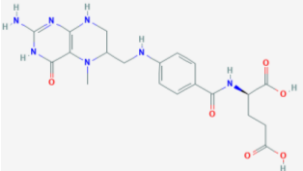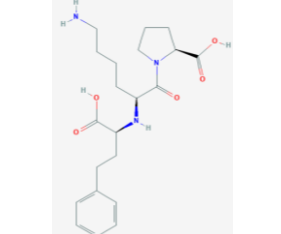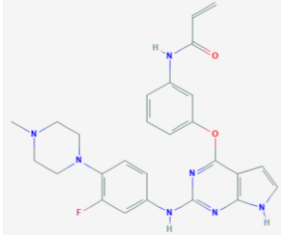
Correspondence to: Marek Štekláč (E-mail: *xsteklacm@stuba.sk*)
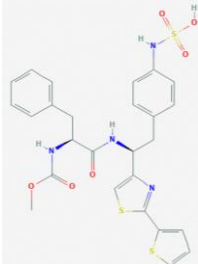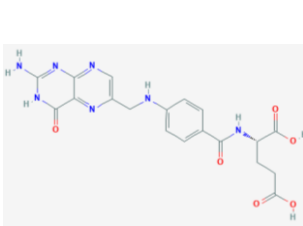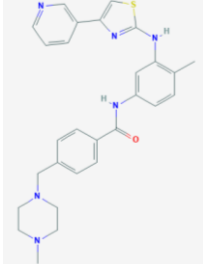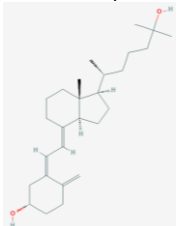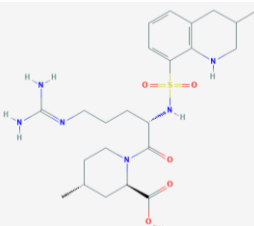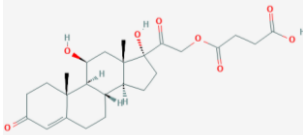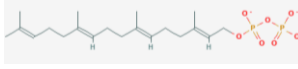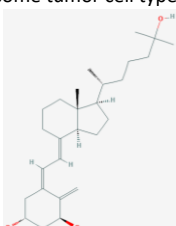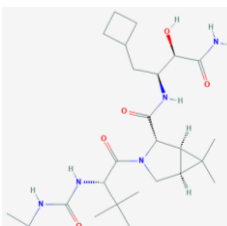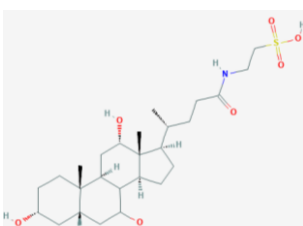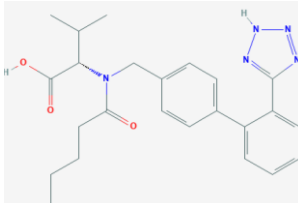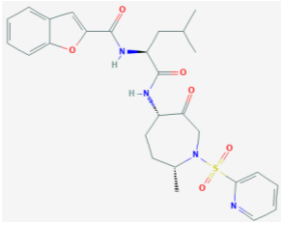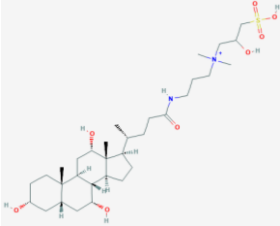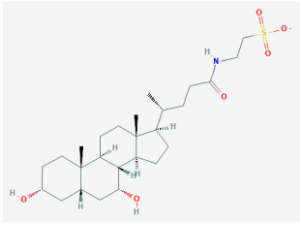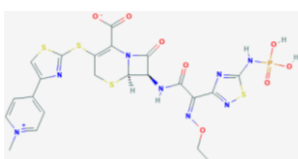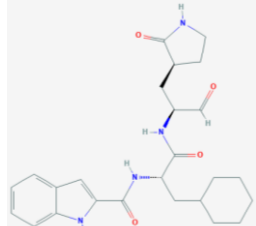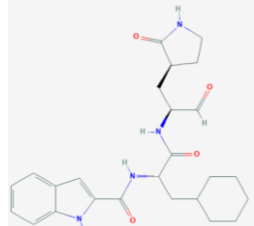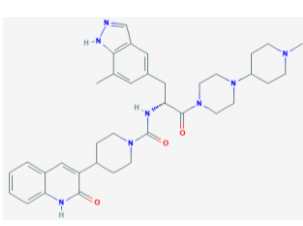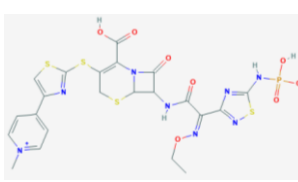
[1] *Institute of Physical Chemistry and Chemical Physics, Faculty of Chemical and Food Technology, Slovak Technical University, SK-81237, Bratislava, Slovakia*

TABLE OF CONTENTS

Table S1. CID identifiers, trivial names (in brackets), docking scores in kcal/mol, recognized pharmacological functions and molecular structures[1] of ten compounds downloaded PubChem database [2,3] with highest binding affinities towards 3CL^{pro}/PL^{pro} structures.

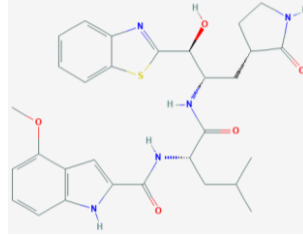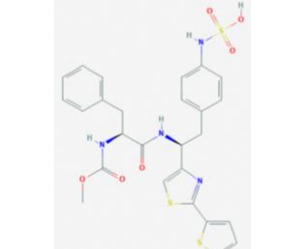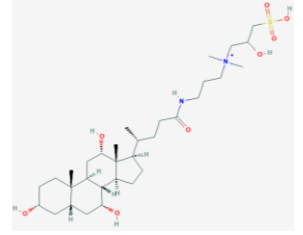| №	6WQF (3CL^{pro})	6LU7 (3CL^{pro})	6WZU (PL^{pro})	7CMD (PL^{pro})
1	5281040 (Montelukast) -14.75 Anti-inflammatory and bronchodilating activity	3191 (Ebastine) -14.11 Anti-inflammatory activity	16923 (Solumedrol) -10.89 Anti-inflammatory and immunosuppressive activity	121893 (Protoporphyrinogen IX) -11.58 -
2	53472683 (Vazegepant/zavegepant) -14.57 Anti-migraine activity	53472683 (Vazegepant/zavegepant) -13.80 Anti-migraine activity	73425380 (TAK-599) -10.69 Anti-MRSA activity	9548902 (Taurochenode oxycholate(1-)) -11.24 Human metabolite
3	6918155 (Ciclesonide) -14.39 Anti-inflammatory and anitiviral activity	154573806 (GRL-024-20) -13.58 - [a]	25245769 (Biliverdine(2-)) -10.67 Human metabolite	60947 (Tirofiban) -10.97 Anti-coagulant activity
4	5459840 (20-Hydroxyecdysone) -14.07 Protective role in the cardiovascular system and performance enhancing activity	5281040 (Montelukast) -12.83 Anti-inflammatory and bronchodilating activity	135483998 (5-Methyltetrahydrofolate) -10.66 Anti-neoplastic and antidepressant activity	5362119 (Lisinopril) -10.90 ACE inhibitor with anti-hypertensive activity
5	154573806 (GRL-024-20) -14.05 - [a]	46700782 (Razuprotafib) -12.83 Potential vasculature stabilizing activity	122146 (-[b]) -10.61 - [a]	72734520 (Avitinib) -10.77 Tyrosine kinase inhibitor

2

6	46700782 (Razuprotafib) -13.86 Potential vasculature stabilizing activity 	71481120 (GC-376) -12.79 Broad-spectrum antiviral drug in development 	135398658 (Folic acid) -10.58 Essential for hematopoiesis and red blood cell production 	10074640 (Masitinib) -10.75 Tyrosine kinase inhibitor
7	5283731 (Calcifediol) -13.78 Vitamin D supplementation with potential immunomodulating activity 	92722 (Argatroban) -12.76 Anti-thrombotic activity 	16623 (-[b]) (Hydrocortisone hemisuccinate) -10.41 Anti-inflammatory and immunosuppressive activity 	5497105 (Geranylgeranyl diphosphate) -10.71 Human metabolite
8	5280453 (Calcitriol) -13.63 Synthetic analogue of vitamin D able to inhibit proliferation of some tumor cell types 	71316139 (-[b]) -12.66 -[a] 	46783527 (Taurocholic acid) -10.40 Human metabolite 	60846 (Valsartan) -10.67 Angiotensin II antagonist with anty-hypertensive activity
9	6918602 (Relacatib) -13.49 Inhibitor of cathepsin K 	122146 (-[b]) -12.57 -[a] 	9548902 (Taurochenodeoxycholate(1-)) -10.37 Human metabolite 	73425380 (TAK-599) -10.56 Anti-MRSA activity
10	145343771 (Peptidomimetic aldehyde 11a) -13.48 Inhibitor of SARS coronavirus main proteinase 	145343771 (Peptidomimetic aldehyde 11a) -12.50 Inhibitor of SARS coronavirus main proteinase 	53472683 (Vazegepant/zavegepant) -10.21 Anti-migraine activity 	9810132 (-[b]) -10.55 -[a]

a) No pharmacological functions have been reported
b) Compound does not have a trivial name

Table S2A. CID, trivial name, docking score (in brackets), putative binding sites and description of predicted H-bonds of five best scoring compounds against 6WQF structure of 3CL^{pro}[4]. Docked compounds are in purple colour and the protein is in green.

5281040 – Montelukast (-14.75 kcal/mol)

His163(NE$_2$) … O$_1$, d = 2.196 Å

H(O$_3$) … Arg188, d = 1.745 Å

Thr190(N)…O$_3$, d = 1.918 Å
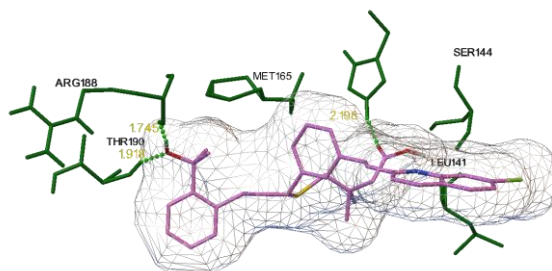
53472683 – Vazegepant (-14.57 kcal/mol)

Thr26(N) … O$_2$, d = 1.818 Å

Asn142(ND$_2$) … O$_3$, d = 2.108 Å
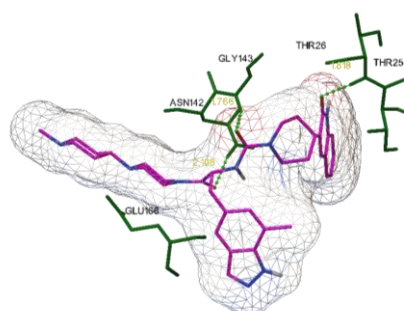
Gly143(N) … O$_1$, d = 1.766 Å

6918155 – Ciclesonide (-14.39 kcal/mol)

Thr26(N) … O$_3$, d = 2.246 Å

Gln189(NE$_2$) … O$_4$, d = 1.803 Å
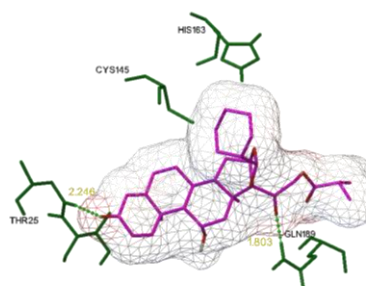
5459840 – 20-hydroxyecdysone (-14.07 kcal/mol)

Thr26(N) … O$_7$, d =1.877 Å

Gly143(N) … O$_1$, d = 1.980 Å

Glu166(N) … O$_2$, d = 1.756 Å

H(O$_2$) … Gu166(O), d = 2.097 Å

Thr190(N) … O$_4$, d = 1.745 Å

H(O$_4$) … Thr190(O), d = 1.812 Å

Gln192(NE) … O$_4$, d = 2.216 Å
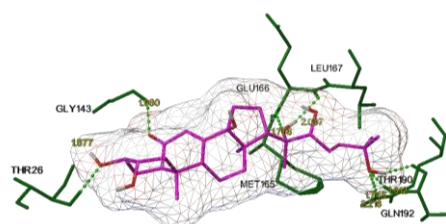
154573806 – GLR-024-20 (-14.05 kcal/mol)

H(N$_5$) … Thr26(O), d = 1.917 Å

H(N$_2$) … Phe140(O), d = 1.983 Å

Gly143(N) … O$_1$, d = 1.995 Å

His163(NE$_2$) … O$_2$, d = 1.996 Å

H(O$_3$) … His164(O), d = 2.247 Å

Glu166(N) … N$_3$, d = 1.824 Å
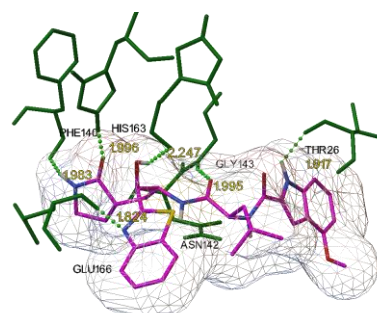
Table S2B. CID, trivial name, docking score (in brackets), putative binding sites and description of predicted H-bonds of five best scoring compounds against 6LU7 structure of 3CL^pro[5]. Docked compounds are in purple colour and the protein is in orange.
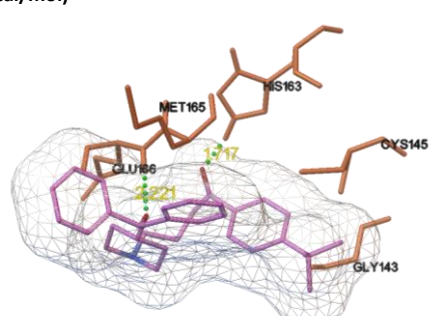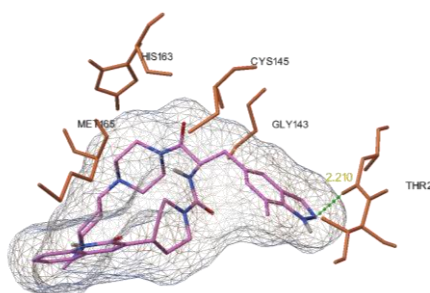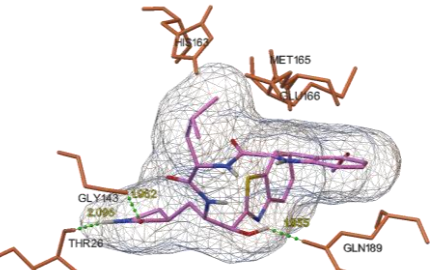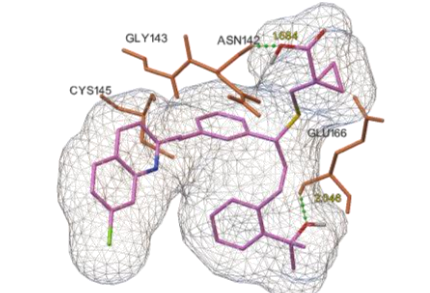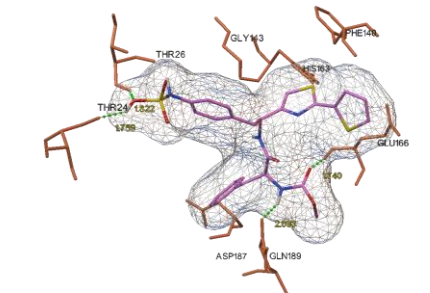
3191 – Ebastine (-14.11 kcal/mol)

His163(NE_2) … O_1, d = 1.717 Å

Glu166(N) … O_2, d = 2.221 Å

53472683 – Vazegepant (-13.80 kcal/mol)

Thr26(N) … N_8, d = 2.210 Å

154573806 – GRL-024-20 (-13.58 kcal/mol)

H(N_2) … Thr26(O), d = 2.095 Å

Gly143(N) … O_2, d = 1.962 Å

H(O_3) … Gln189(OE_1), d = 1.955 Å

5281040 – Montelukast (-12.83 kcal/mol)

Asn142(N) … O_2, d = 1.684 Å

Glu166 … O_3, d = 2.046 Å

46700782 – Razuprotafib (-12.83 kcal/mol)

Thr26(N) … O_4, d =1.822 Å

H(O_4) … Thr24(O), d =1.759 Å

Glu166(N) … O_3, d =1.740 Å

H(N_2) … Gln189(OE_1), d = 2.033 Å

Table S2C. CID, trivial name, docking score (in brackets), putative binding sites and description of predicted H-bonds of five best scoring compounds against 6WZU structure of PL^{pro}[6]. Docked compounds are in purple colour and the protein is in blue.

16923 – Solumedrol (-10.89 kcal/mol)

Lys105(NZ) … O$_7$, d = 1.721 Å

Trp106(N) … O$_5$, d = 1.884 Å

H(O$_2$) … Asp286(OD$_1$), d = 2.081 Å

Ala288(N) … O$_5$, d = 1.852 Å
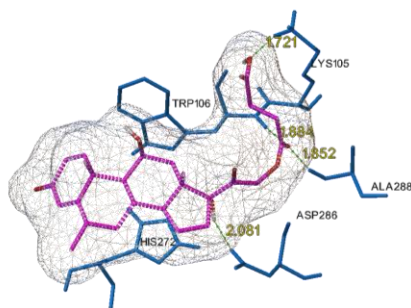
73425380 – TAK-599 (-10.69 kcal/mol)

His89(ND$_1$) … O$_5$, d = 2.062 Å

Lys105(NZ) … O$_1$, d = 1.831 Å

Asp108(N) … O$_3$, d = 1.694 Å

H(O$_4$) … Asp108(OD$_2$), d = 1.752 Å

H(O$_6$) … Asp108(OD$_2$), d = 2.014 Å
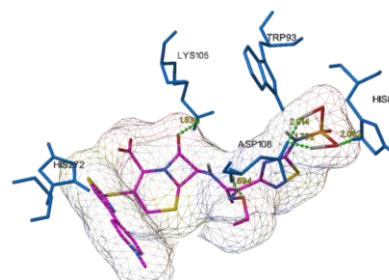
25245769 – Biliverdin(2-) (-10.67 kcal/mol)

Lys105(NZ) … O$_3$, d = 1.720 Å

H(N$_2$) … Trp106(O), d = 1.912 Å

Asp108(N) … O$_6$, d = 2.082 Å

Ala288(N) … O$_3$, d = 1.662 Å
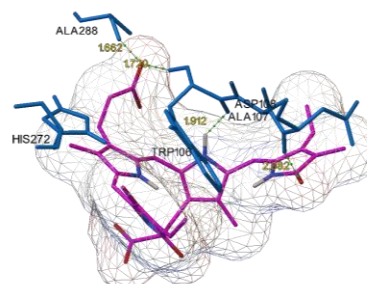
135483998 – 5-Methyltetrahydrofolate (-10.66 kcal/mol)

Lys105(NZ) … O$_4$, d = 1.985 Å

Trp106(N) … O$_5$, d = 1.579 Å

H(N$_5$) … Asn109(OD$_1$), d = 2.092 Å

H(N$_6$) … Asn109(OD$_1$), d = 2.130 Å

Ala288(N) … O$_5$, d = 1897 Å
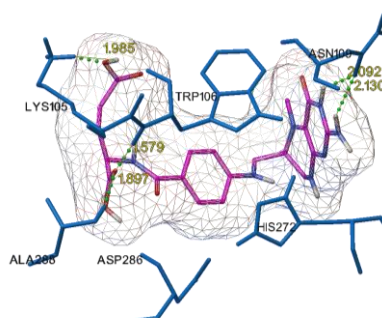
122146 (-10.61 kcal/mol)

Trp106(N) … (O$_4$), d = 1.768 Å

Asn109(ND$_2$) … (O$_7$), d = 1.808 Å

H(O$_6$) … Asn109(OD$_1$), d = 2.154 Å

H(O$_8$) … Gly160(O), d = 2.109 Å

H(O$_5$) … Asp286(O), d = 2.042 Å

Ala288(N) … O$_5$, d = 2.210 Å
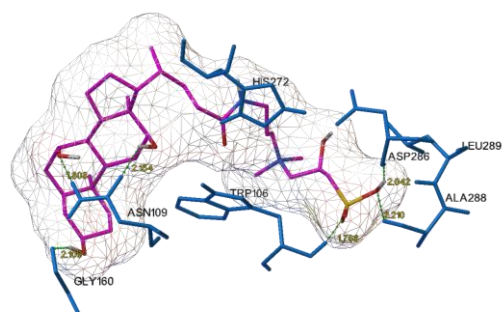
Table S2D. CID, trivial name, docking score (in brackets), putative binding sites and description of predicted H-bonds of five best scoring compounds against 7CMD structure of PL[pro] [7]. Docked compounds are in purple colour and the protein is in yellow.


121893 – Protoporphyrinogen IX (-11.58 kcal/mol)

Lys105(NZ) … O_1, d = 1.972 Å

Trp106(NZ) … O_2, d = 1.987 Å
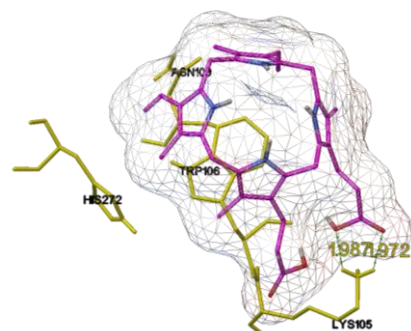
9548902 – Taurochenode oxycholate(1-) (-11.24 kcal/mol)

Lys105(NZ) … O_6, d = 2.179 Å

H(O_6) … Trp106(O), d = 2.109 Å

Asn267(ND) … O_2, d = 2.022 Å

Asn267(N) … O_3, d = 1.855 Å

H(N) … Cys270(O), d = 1.951 Å
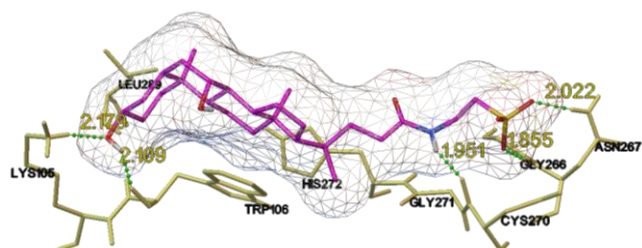
60947 – Tirofiban (-10.97 kcal/mol)

H(N_2) … Cys270(O), d = 2.151 Å

His272(NE_2) … O_1, d = 2.166 Å

H(N_1) … Asp286(O), d = 2.180 Å

Ala288(N) … O_3, d = 2.160 Å
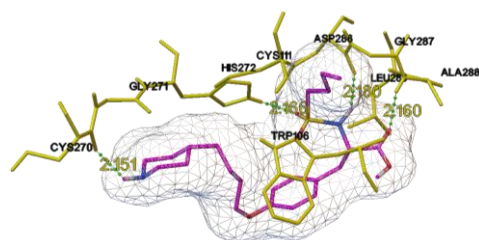
5362119 – Lisinopril (-10.90 kcal/mol)

Lys105(NZ) … O_4, d = 2.135 Å

H(N_3) … Tyr273(O), d = 2.002 Å

H(N_3) … Asp286 (OD_1), d = 1.689 Å
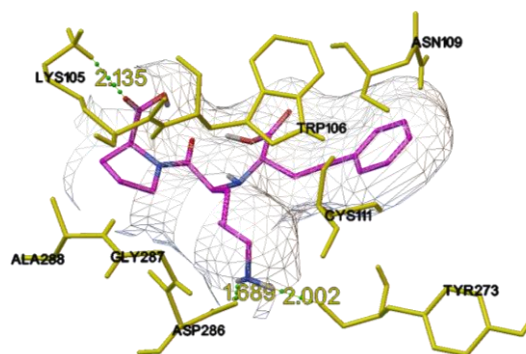
72734520 – Avitinib (-10.77 kcal/mol)

H(N_7) … Asp286(OD_1), d = 2.053 Å
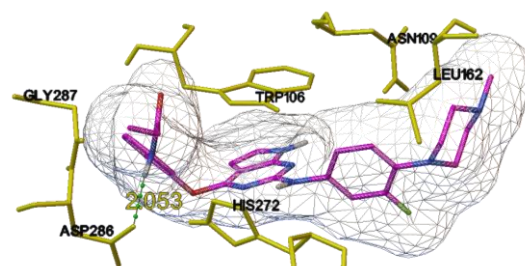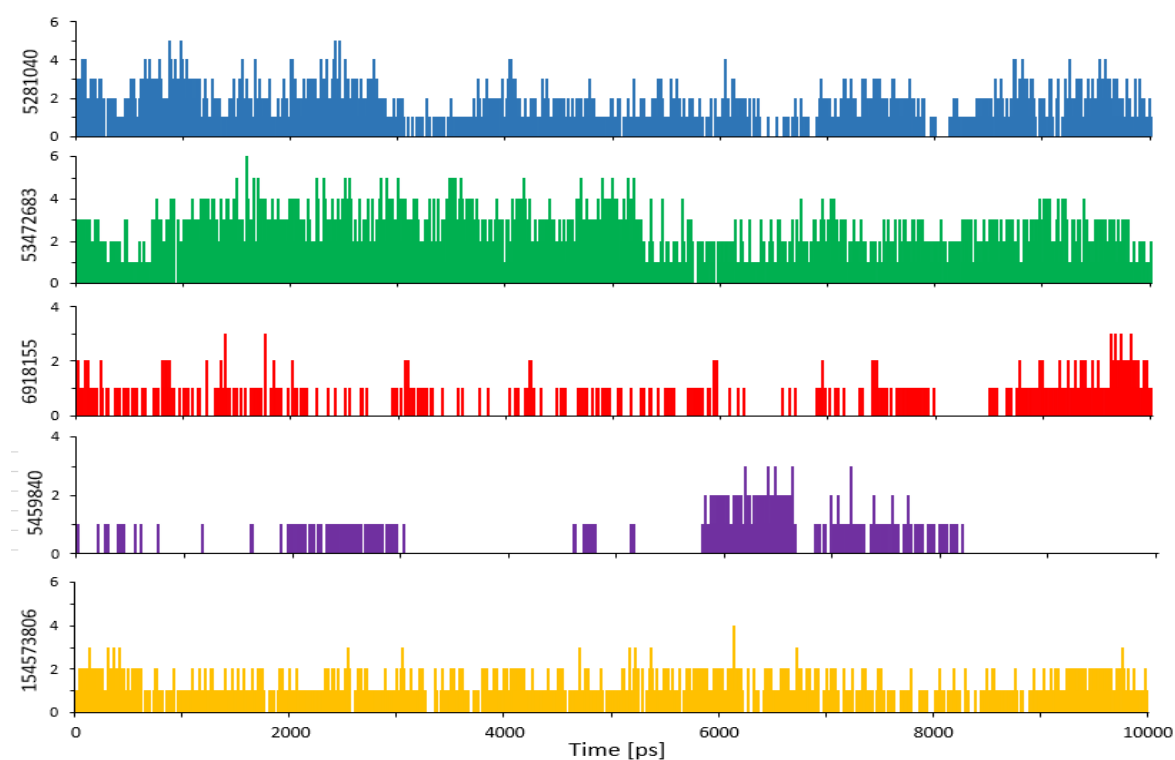
Figure S1A. Time plot evolution of H-bonds formed between 6WQF 3CL^pro structure and Montelukast (CID: 5281040) represented by blue colour, Vazegepant/zevagepant (CID: 53472683) represented by green colour, Ciclesonide (CID: 6918155) represented by red colour, 20-hydroxyecdysone (CID: 5459840) represented by violet colour and GRL-024-20 (CID: 154573806) represented by yellow colour.
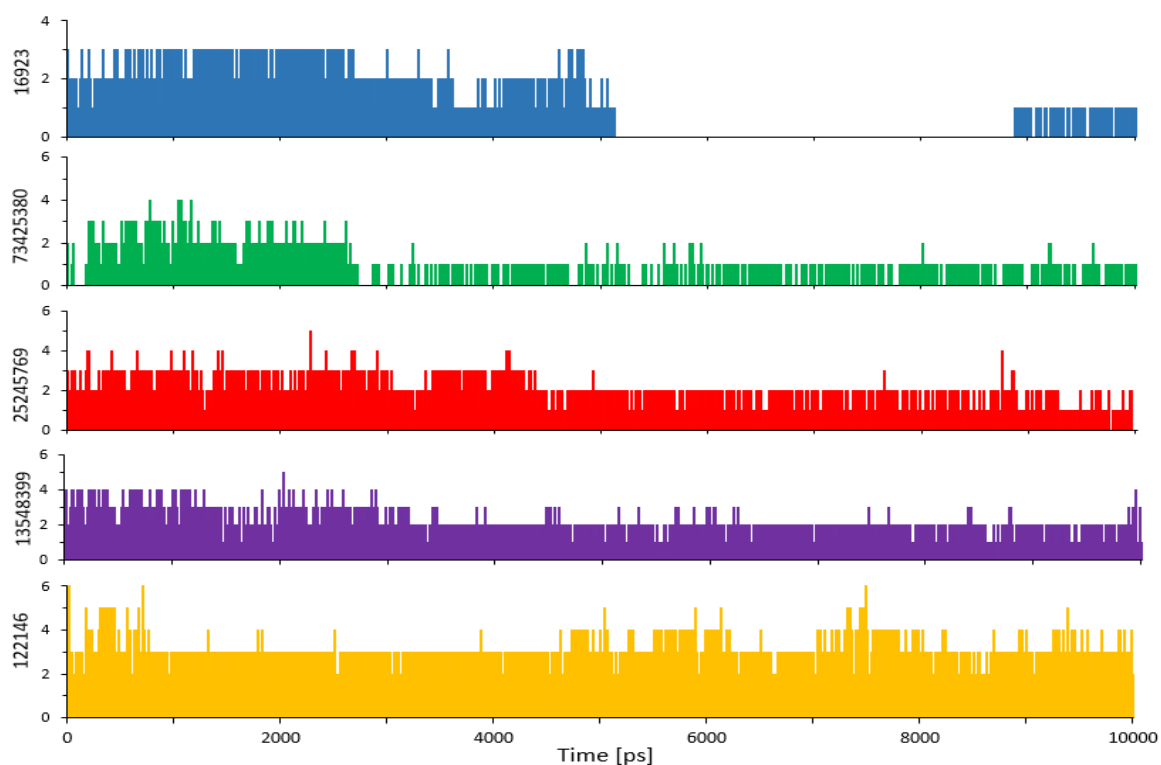
Figure S1B. Time plot evolution of H-bonds formed between 6WZU PL^pro structure and Solumedrol (CID: 16923) represented by blue colour, TAK-599 (CID: 73425380) represented by green colour, Biliverdine(2-) (CID: 25245769) represented by red colour, 5-Methyltetrahydrofolate (CID: 135483998) represented by violet and compound CID: 122146 represented by yellow colour.

Table S3A. H-bonds identifications and their occupancy over the MD simulation of 5281040 (Montelukast)-6WQF complex with 1 % time cut-off.

Donor atom	Acceptor atom	Occupancy
Lig-O_3	Thr190-Main-O	42.12%
Lig-O_2	Ser144-Side-OG	32.04%
Glu166-Main-N	Lig-S	20.16%
His163-Side-NE_2	Lig-O_1	12.28%
Gln192-Main-N	Lig-O_3	9.98%
His163-Side-NE_2	Lig-O_2	7.68%
Ser144-Main-N	Lig-O_1	6.69%
Lig-O_2	His164-Main-O	5.39%
Glu166-Main-N	Lig-O_1	3.59%
Glu143-Main-N	Lig-O_1	1.50%
Glu166-Main-N	Lig-O_2	1.00%

Table S3B. H-bonds identifications and their occupancy over the MD simulation of 53472683 (Vazegepant)-6WQF complex with 1 % time cut-off.

Donor atom	Acceptor atom	Occupancy
Thr26-Main-N	Lig-O_2	72.95%
Lig-N_3	Thr24-Main-O	33.13%
Gly143-Main-N	Lig-O_1	30.84%
Gln189-Side-NE_2	Lig-N_8	29.64%
Cys145-Main-N	Lig-O_1	22.65%
Asn142-Side-ND_2	Lig-O_1	10.28%
Ser144-Main-N	Lig-O_1	6.29%
Lig-N7	Gln189-Side-OE_1	4.79%
Asn142-Side-ND_2	Lig-O_3	2.69%
Gln189-Side-NE_2	Lig-N_7	2.30%
Thr25-Side-OG_1	Lig-O_2	1.20%
Cys145-Side-SG	Lig-N_2	1.10%

Table S3C. H-bonds identifications and their occupancy over the MD simulation of 6918155 (Ciclesonide)-6WQF complex with 1 % time cut-off.

Donor atom	Acceptor atom	Occupancy
Arg4-Side-NH_2	Lig-O_2	9.68%
Lys5-Side-NZ	Lig-O_4	6.39%
Arg4-Side-NE	Lig-O_4	3.29%
Ala285-Main-N	Lig-O_7	3.09%
Arg4-Side-NH_2	Lig-O_4	2.79%
Arg4-Side-NH_2	Lig-O_7	1.30%
Lig-O_7	Val125-Main-O	1.20%
Arg4-Side-NE	Lig-O_2	1.20%
Thr280-Side-OG_1	Lig-O_5	1.10%

Table S3D. H-bonds identifications and their occupancy over the MD simulation of 5459840 (20-hydroxyecdysone)-6WQF complex with 1 % time cut-off.

Donor atom	Acceptor atom	Occupancy
Thr26-Main-N	Lig-O_3	10.68%
Ser46-Side-OG	Lig-O_7	9.38%
Gln189-Side-NE_2	Lig-O_4	7.98%
Glu166-Main-N	Lig-O_2	3.99%
Lig-O_7	Gln189-Side-OE_1	3.59%
Thr190-Main-N	Lig-O_6	1.80%
Gln189-Side-NE_2	Lig-O_6	1.70%
Lig-O_7	Ser46-Side-OG	1.20%

Table S3E. H-bonds identifications and their occupancy over the MD simulation of 154573806 (GRL-024-20)-6WQF complex with 1 % time cut-off.

Donor atom	Acceptor atom	Occupancy
Asn142-Side-ND_2	Lig-O_1	24.55%
Lig-N_2	Asn142-Side-OD_1	19.46%
Glu166-Main-N	Lig-O_3	17.76%
Glu166-Main-N	Lig-S	15.37%
Gly143-Main-N	Lig-O_1	6.49%
Lig-N_4	Ser46-Side-OG	3.79%
His41-Side-NE_2	Lig-O_4	2.89%
Gly143-Main-N	Lig-O_4	1.60%
Gly143-Main-N	Lig-O_2	1.10%

Table S4A. H-bonds identifications and their occupancy over the MD simulation of 16923 (Solumedrol)-6WZU complex with 1 % time cut-off.

Donor atom	Acceptor atom	Occupancy
Lig-O_5	Asp286-Side-OD_1	87.24%
Lig-O_2	Asp286-Side-OD_2	85.95%
Trp106-Main-N	Lig-O_4	75.98%
Ala288-Main-N	Lig-O_3	12.97%
Lig-O_2	Asp286-Side-OD_1	5.38%
Lig-O_8	Asn109-Side-OD_1	3.79%
Lys274-Side-NZ	Lig-O_1	2.90%
Asn267-Side-ND_2	Lig-O_6	2.70%
Lig-O_6	Asn267-Side-OD_1	1.89%
Lig-O_8	Asn267-Side-OD_1	1.60%
Lig-O_6	Asn267-Main-O	1.10%
Trp106-Main-N	Lig-O_5	1.10%

Table S4B. H-bonds identifications and their occupancy over the MD simulation of 73425680 (TAK-599)-6WZU complex with 1 % time cut-off.

Donor atom	Acceptor atom	Occupancy
Lig-O_6	Asp286-Main-O	88.72%
Ala288-Main-N	Lig-O_5	81.23%
Lig-N_6	Gly271-Main-O	12.65%
Lig-N_6	Asn109-Side-OD_1	7.97%
Lig-N_5	Asn109-Side-OD_1	2.99%
Lig-N_3	Cys270-Main-O	2.79%
LYS105-Side-NZ	Lig-O_3	1.60%
Lig-N_6	Gln269-Main-O	1.60%

Table S4C. H-bonds identifications and their occupancy over the MD simulation of 25245769 (Biliverdine(2-))-6WZU complex with 1 % time cut-off.

Donor atom	Acceptor atom	Occupancy
Ala288-Main-N	Lig-O_3	58.62%
Trp106-Main-N	Lig-O_2	45.07%
Lig-N_1	Trp106-Main-O	35.06%
Trp106-Main-N	Lig-O_3	26.02%
Ala288-Main-N	Lig-O_2	10.37%
Asp108-Main-N	Lig-O_6	4.58%
Lys105-Side-NZ	Lig-O_3	1.70%

Table S4D. H-bonds identifications and their occupancy over the MD simulation of 135483998 (5-methyltetrahydrofolate)-6WZU complex with 1 % time cut-off.

Donor atom	Acceptor atom	Occupancy
Ala288-Main-N	Lig-O_5	42.83%
Lig-O_2	Asp286-Side-OD_1	29.68%
Trp106-Main-N	Lig-O_6	10.66%
Glu252-Main-N	Lig-O_1	7.19%
Trp106-Main-N	Lig-O_2	6.58%
Trp106-Main-N	Lig-O_5	5.08%
Lig-O_2	Asp286-Side-OD_2	3.79%
Lys105-Side-NZ	Lig-O_6	1.80%

Table S4E. H-bonds identifications and their occupancy over the MD simulation of 122146-6WZU complex with 1 % time cut-off.

Donor atom	Acceptor atom	Occupancy
Lys94-Side-NZ	Lig-O_5	27.44%
Lig-O_4	Asp108-Side-OD_2	20.82%
Lig-O_6	Asp108-Side-OD_1	14.15%
Lig-O_4	Lys92-Main-O	7.68%
Asp108-Main-N	Lig-O_3	3.69%
Lig-N_6	Asp108-Side-OD_1	3.59%
Lys105-Side-NZ	Lig-O_1	1.99%
Lys105-Side-NZ	Lig-O_2	1.20%
Lig-O_6	Lys92-Main-O	1.20%
Lig-O_6	Asp108-Side-OD_2	1.20%
Lig-O_4	Asp108-Side-OD_1	1.10%
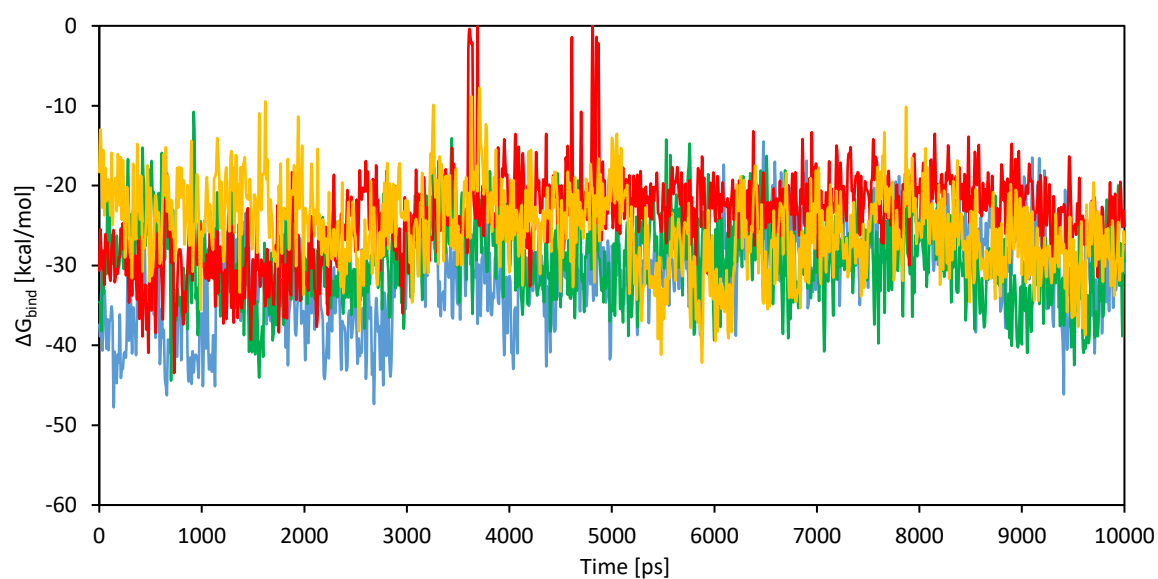
Figure S2A. Time plot evolution of binding free energies values calculated using MM-PBSA approach (Molecular Mechanics – Poisson-Boltzmann Surface Area)[8,9] of complexes with 6WQF 3CL^{pro} structure. Montelukast (CID: 5281040) represented by blue colour, Vazegepant/zevagepant (CID: 53472683) represented by green colour, Ciclesonide (CID: 6918155) represented by red colour and GRL-024-20 (CID: 154573806) represented by yellow colour.
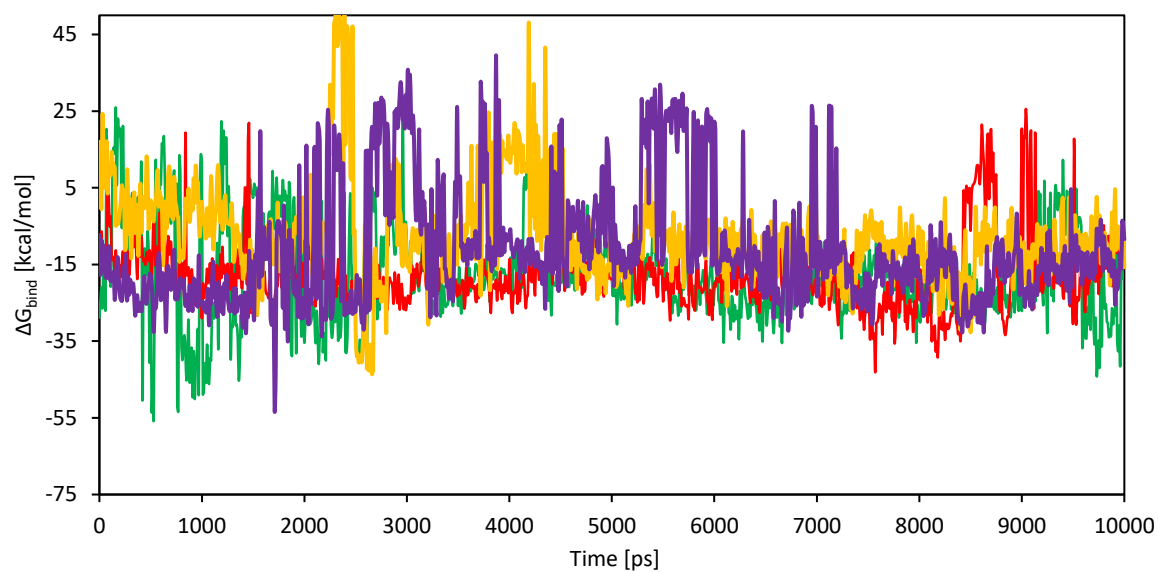
Figure S2B. Time plot evolution of binding free energies values calculated using MM-PBSA approach[8,9] of complexes with 6WZU PLpro structure. TAK-599 (CID: 73425380) represented by green colour, Biliverdine(2-) (CID: 25245769) represented by red colour, 5-methyltetrahydrofolate (CID: 135483998) represented by violet and compound CID: 122146 represented by yellow colour.

Figure S3. Docking pose of Suramine (CID: 5361) in the 6WZU PL^pro structure. Cyclisation of the compound is illustrated by the intramolecular distances of atoms that are suspected to participate in H-bonds formation.

A

B

C

D

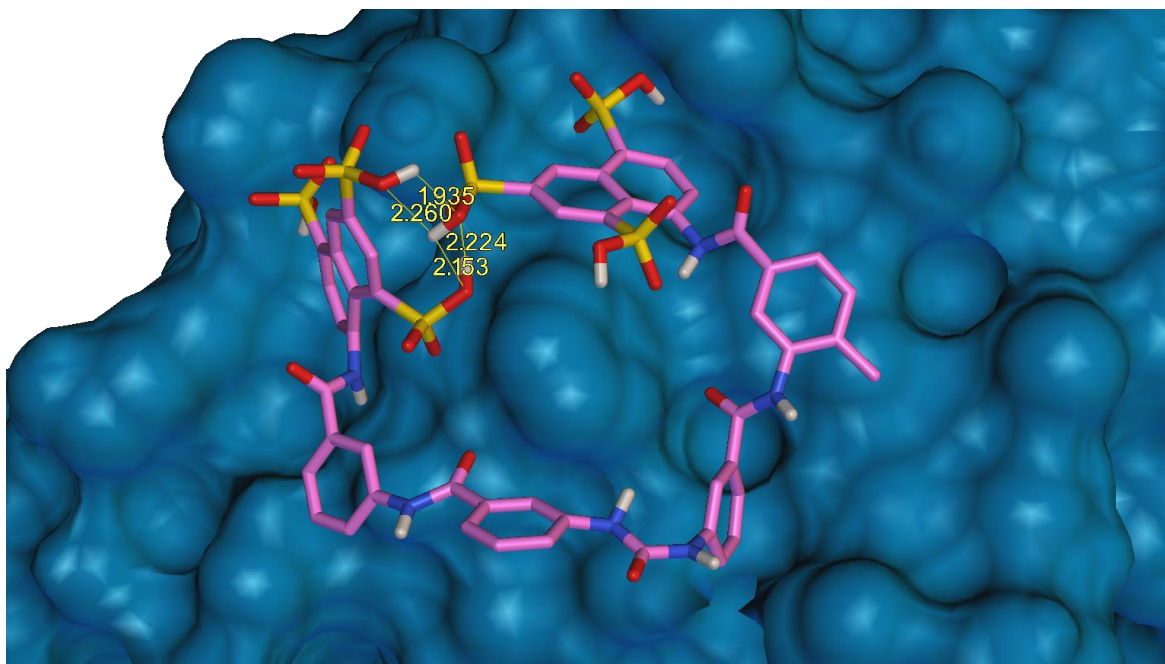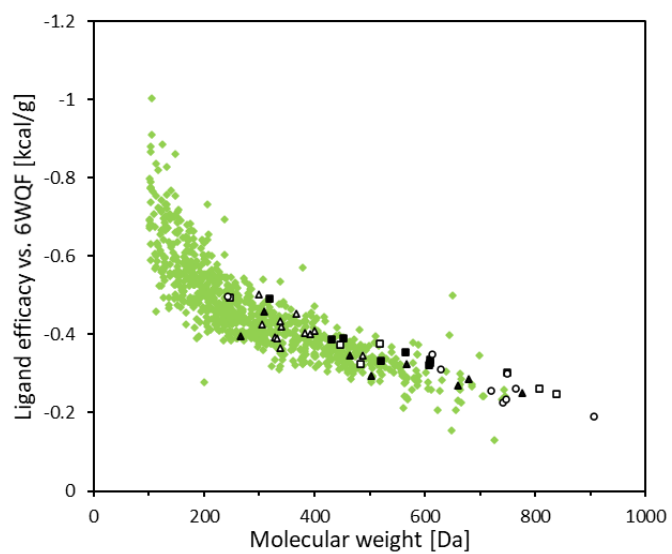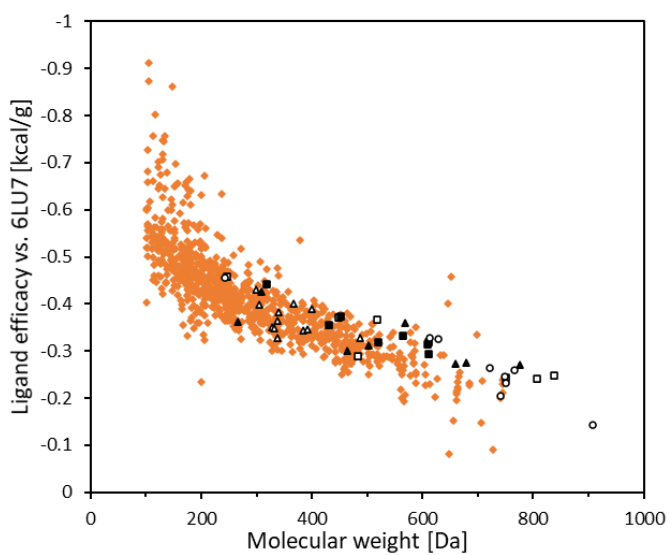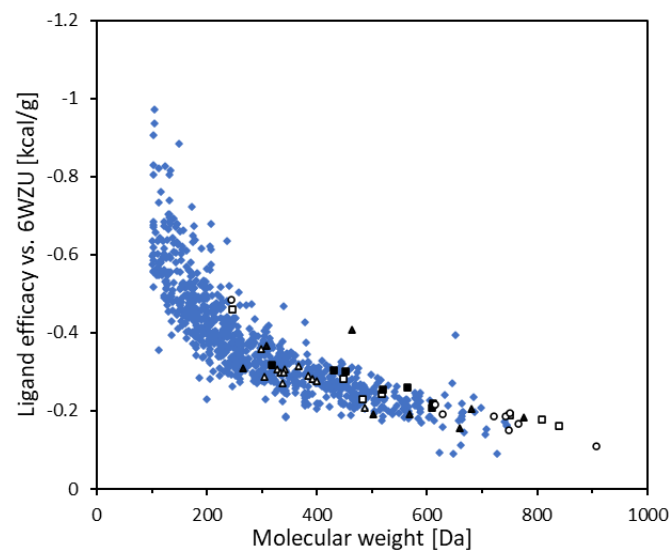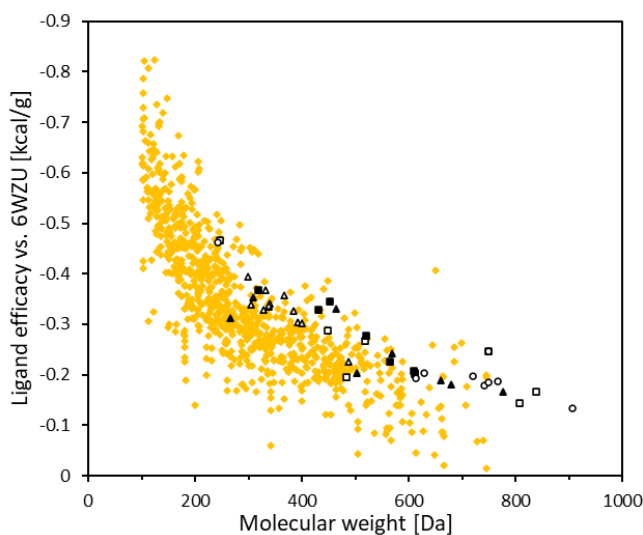**Figure S4.** Ligand efficacies of initially selected compounds (colored diamonds), redocked compounds from selected publications (empty triangles) [10], (full triangles) [11], (empty squares) [12], (full squares) [13] and (empty circles) [14] against 6WQF (A), 6LU7 (B), 6WZU (C) and 7CMD (D) with respect to their molecular weight. Compounds with molecular weight exceeding 1000 Da, one from Wu *et al.* [11] (CID: 5361) and one from Shah *et al.* [14] (CID: 123794), are excluded from these representations.

References

[1]   2D structure image of CID 122146, (n.d.). https://pubchem.ncbi.nlm.nih.gov/compound/122146#section=2D-Structure (accessed December 1, 2020).

[2]   S. Kim, J. Chen, T. Cheng, A. Gindulyte, J. He, S. He, Q. Li, B.A. Shoemaker, P.A. Thiessen, B. Yu, L. Zaslavsky, J. Zhang, E.E. Bolton, PubChem 2019 update: improved access to chemical data, Nucleic Acids Res. 47 (2018) D1102–1109. https://doi.org/10.1093/nar/gky1033.

[3]   S. Kim, J. Chen, T. Cheng, A. Gindulyte, J. He, S. He, Q. Li, B.A. Shoemaker, P.A. Thiessen, B. Yu, L. Zaslavsky, J. Zhang, E.E. Bolton, PubChem in 2021: new data content and improved web interfaces, Nucleic Acids Res. 49 (2021) D1388–D1395. https://doi.org/10.1093/nar/gkaa971.

[4]   D.W. Kneller, G. Phillips, H.M. O'Neill, R. Jedrzejczak, L. Stols, P. Langan, A. Joachimiak, L. Coates, A. Kovalevsky, Structural plasticity of SARS-CoV-2 3CL Mpro active site cavity revealed by room temperature X-ray crystallography, Nat. Commun. 11 (2020) 3202. https://doi.org/10.1038/s41467-020-16954-7.

[5]   Z. Jin, X. Du, Y. Xu, Y. Deng, M. Liu, Y. Zhao, B. Zhang, X. Li, L. Zhang, C. Peng, Y. Duan, J. Yu, L. Wang, K. Yang, F. Liu, R. Jiang, X. Yang, T. You, X. Liu, X. Yang, F. Bai, H. Liu, X. Liu, L.W. Guddat, W. Xu, G. Xiao, C. Qin, Z. Shi, H. Jiang, Z. Rao, H. Yang, Structure of Mpro from SARS-CoV-2 and discovery of its inhibitors, Nature. 582 (2020) 289–293. https://doi.org/10.1038/s41586-020-2223-y.

[6]   J. Osipiuk, S.-A. Azizi, S. Dvorkin, M. Endres, R. Jedrzejczak, K.A. Jones, S. Kang, R.S. Kathayat, Y. Kim, V.G. Lisnyak, S.L. Maki, V. Nicolaescu, C.A. Taylor, C. Tesar, Y.-A. Zhang, Z. Zhou, G. Randall, K. Michalska, S.A. Snyder, B.C. Dickinson, A. Joachimiak, Structure of papain-like protease from SARS-CoV-2 and its complexes with non-covalent inhibitors, BioRxiv. (2020) 2020.08.06.240192. https://doi.org/10.1101/2020.08.06.240192.

[7]   X. Gao, B. Qin, P. Chen, K. Zhu, P. Hou, J.A. Wojdyla, M. Wang, S. Cui, Crystal structure of SARS-CoV-2 papain-like protease, Acta Pharm. Sin. B. 11 (2021) 237–245. https://doi.org/https://doi.org/10.1016/j.apsb.2020.08.014.

[8]   R. Kumari, R. Kumar, A. Lynn, g_mmpbsa—A GROMACS Tool for High-Throughput MM-PBSA Calculations, J. Chem. Inf. Model. 54 (2014) 1951–1962. https://doi.org/10.1021/ci500020m.

[9]   N.A. Baker, D. Sept, S. Joseph, M.J. Holst, J.A. McCammon, Electrostatics of nanosystems: Application to microtubules and the ribosome, Proc. Natl. Acad. Sci. 98 (2001) 10037–10041. https://doi.org/10.1073/pnas.181342398.

[10] A. Fischer, M. Sellner, S. Neranjan, M.A. Lill, M. Smieško, Inhibitors for Novel Coronavirus Protease Identified by Virtual Screening of 687 Million Compounds, (2020). https://doi.org/10.26434/chemrxiv.11923239.v1.

[11] C. Wu, Y. Liu, Y. Yang, P. Zhang, W. Zhong, Y. Wang, Q. Wang, Y. Xu, M. Li, X. Li, M. Zheng, L. Chen, H. Li, Analysis of therapeutic targets for SARS-CoV-2 and discovery of potential drugs by computational methods, Acta Pharm. Sin. B. 10 (2020) 766–788. https://doi.org/https://doi.org/10.1016/j.apsb.2020.02.008.

[12] F.S. Hosseini, M. Amanlou, Anti-HCV and anti-malaria agent, potential candidates to repurpose for coronavirus infection: Virtual screening, molecular docking, and molecular dynamics simulation study, Life Sci. 258 (2020) 118205. https://doi.org/https://doi.org/10.1016/j.lfs.2020.118205.

[13] S. Adem, V. Eyupoglu, I. Sarfraz, A. Rasul, M. Ali, Identification of Potent COVID-19 Main Protease (Mpro) Inhibitors from Natural Polyphenols: An in Silico Strategy Unveils a Hope against CORONA, (2020). https://doi.org/10.20944/PREPRINTS202003.0333.V1.

[14] B. Shah, P. Modi, S.R. Sagar, In silico studies on therapeutic agents for COVID-19: Drug repurposing approach., Life Sci. 252 (2020) 117652. https://doi.org/10.1016/j.lfs.2020.117652.